

Weak Corrections to Three-Jet Production in Electron-Positron Annihilations: 1) The Factorisable Contributions*

E. Maina

Dipartimento di Fisica Teorica – Università di Torino
Via Pietro Giuria 1, 10125 Torino, Italy
and
Istituto Nazionale di Fisica Nucleare – Sezione di Torino
Via Pietro Giuria 1, 10125 Torino, Italy
E-mail: maina@to.infn.it

S. Moretti

CERN – Theory Division
CH-1211 Geneva 23, Switzerland
and
Institute for Particle Physics Phenomenology – University of Durham
South Road, Durham DH1 3LE, UK
E-mails: stefano.moretti@cern.ch, stefano.moretti@durham.ac.uk

D.A. Ross

Department of Physics and Astronomy – University of Southampton
Highfield, Southampton SO17 1BJ, UK
Email: dar@hep.phys.soton.ac.uk

ABSTRACT: We report on the calculation of the factorisable one-loop weak-interaction corrections to the initial and final states for three-jet observables in electron-positron annihilations. We show that such corrections are of a few percent at $\sqrt{s} = M_Z$. Hence, while their impact is not dramatic in the context of LEP1 and SLC, where the total error on the measured value of α_S is larger, at a future Linear Collider, running at the Z mass peak (e.g., GigaZ), they ought to be taken into account in the experimental fits, as here the uncertainty on the value of the strong coupling constant is expected to be at the 0.1% level or even smaller. The calculation has been performed using helicity amplitudes so that it can be applied to the case of polarised beams.

KEYWORDS: QCD processes, Electroweak effects, Loop calculations, Lepton colliders.

Contents

1. Electroweak corrections at high energies	1
2. One-loop weak effects in three-jets events at leptonic colliders	2
3. Calculation	3
4. Numerical results	7
5. Conclusions	11

1. Electroweak corrections at high energies

Strong (QCD) and Electroweak (EW) interactions are two fundamental forces of Nature, the latter in turn unifying weak and electromagnetic (EM) interactions. Together they constitute the Standard Model (SM) of particle physics. A clear hierarchy exists between the strengths of the two interactions at the energy scales probed by past and present high energy particle accelerators (e.g., LEP, SLC, HERA, RHIC and Tevatron) or, indeed, at a future generation electron-positron Linear Collider (LC) [1], running with very high luminosity at $\sqrt{s} = M_Z$ (the so-called ‘GigaZ’ stage, where s is the collider CM energy squared): QCD forces are stronger than EW ones. This is quantitatively manifest if one recalls that the value of the QCD coupling ‘constant’, α_S , measured at these machines is much larger than the EW one, α_{EW} , typically, by an order of magnitude.

A peculiar feature distinguishing QCD and EW effects in higher orders is that the latter are enhanced by double logarithmic factors, $\log^2(\frac{s}{M_W^2})$, which, unlike in the former, do not cancel for ‘infrared-safe’ observables [2] – [4]. The origin of these ‘double logs’ is understood. It is due to a lack of cancellation of infrared (both soft and collinear) virtual and real emission in higher order contributions. This is in turn a consequence of the violation of the Bloch-Nordsieck theorem in non-Abelian theories [5]¹. The problem is in principle present also in QCD. In practice, however, it has no observable consequences, because of the final averaging of the colour degrees of freedom of partons, forced by their confinement into colourless hadrons. This does not occur in the EW case, where, e.g., the

*Work supported in part by the U.K. Particle Physics and Astronomy Research Council (PPARC), by the European Union (EU) under contract HPRN-CT-2000-00149 and by the Italian Ministero dell’Istruzione, dell’Università e della Ricerca (MIUR) under contract 2001023713_006.

¹Recently, it has been found that Bloch-Nordsieck violation can also occur in spontaneously broken Abelian gauge theories, if the incoming particles are mass eigenstates that do not coincide with gauge eigenstates [6]. In the SM this is particularly relevant for incoming longitudinal gauge bosons or Higgs scalars [7].

initial state has a non-Abelian charge, dictated by the given collider beam configuration, such as in e^+e^- collisions.

These logarithmic corrections are finite (unlike in QCD), as the masses of the EW gauge bosons provide a physical cut-off for W and Z emission. Hence, for typical experimental resolutions, softly and collinearly emitted weak bosons need not be included in the production cross-section and one can restrict oneself to the calculation of weak effects originating from virtual corrections and affecting a purely hadronic final state. Besides, these contributions can be isolated in a gauge-invariant manner from EM effects [4], [8] – [12], at least in some simple cases (including the process $e^+e^- \rightarrow \gamma^*, Z \rightarrow \text{jets}$ considered here) and therefore may or may not be included in the calculation, depending on the observable being studied. (See Refs. [8] – [33] for a collection of papers dealing with resummed, one- and two-loop EW corrections to various high energy processes.)

2. One-loop weak effects in three-jets events at leptonic colliders

It is the aim of our paper to report on the computation of one-loop weak effects entering three-jet production in electron-positron annihilation at $\sqrt{s} = M_Z$ via the subprocess $e^+e^- \rightarrow \gamma^*, Z \rightarrow \bar{q}qg^2$, when the higher order effects arise only from initial or final state interactions. These represent the so-called ‘factorisable’ corrections, i.e., those involving loops not connecting the initial leptons to the final quarks, which are the dominant ones at $\sqrt{s} = M_Z$ (where the width of the Z resonance provides a natural cut-off for off-shellness effects). The remainder, ‘non-factorisable’ corrections, while being negligible at $\sqrt{s} = M_Z$, are expected to play a quantitatively relevant role as \sqrt{s} grows larger. (The study of the full set of one-loop weak corrections will be the subject of a future publication.) As a whole, one-loop weak effects will become comparable to QCD ones at future LCs running at TeV energy scales³. In contrast, at the Z mass peak, where no logarithmic enhancement occurs, one-loop weak effects are expected to appear at the percent level, hence being of limited relevance at LEP1 and SLC, where the final error on α_S is of the same order or larger [36], but of crucial importance at a GigaZ stage of a future LC, where the relative accuracy of α_S measurements is expected to be at the 0.1% level or smaller [37]. On the subject of higher order QCD effects, it should be mentioned here that a great deal of effort has recently been devoted to evaluate two-loop contributions to the three-jet process (albeit, only at the amplitude level so far, as there are no numerical results available yet) while the one-loop QCD results have been known for some time [38]. Even though a full $\mathcal{O}(\alpha_S^3)$ analysis is not yet available, one can reasonably argue that at $\sqrt{s} = M_Z$ the two-loop QCD corrections should be comparable to the one-loop weak effects computed here.

In the case of e^+e^- annihilations, the most important QCD quantity to be extracted from multi-jet events is precisely α_S . The confrontation of the measured value of the

²See Ref. [34] for the corresponding weak corrections to the Born process $e^+e^- \rightarrow \bar{q}q$ and Ref. [35] for the $\sim n_f$ component of those to $e^+e^- \rightarrow \bar{q}qgg$ (where n_f represents the number of light flavours). For two-loop results on the former, see [22].

³For example, at one-loop level, in the case of the inclusive cross-section of e^+e^- into hadrons, the QCD corrections are of $\mathcal{O}(\frac{\alpha_S}{\pi})$, whereas the EW ones are of $\mathcal{O}(\frac{\alpha_{EW}}{4\pi} \log^2 \frac{s}{M_W^2})$, where s is the collider CM energy squared, so that at $\sqrt{s} = 1.5$ TeV the former are identical to the latter, of order 9% or so.

strong coupling constant with that predicted by the theory through the renormalisation group evolution is an important test of the SM or else an indication of new physics, whose typical mass scale is larger than the collider energy, but which can manifest itself through virtual effects. Jet-shape observables, which offer a handle on non-perturbative QCD effects via large power corrections, would be affected as well.

A further aspect that should be recalled is that weak corrections naturally introduce parity-violating effects in jet observables, detectable through asymmetries in the cross-section, which are often regarded as an indication of physics beyond the SM. These effects are further enhanced if polarisation of the incoming beams is exploited. The option of exploiting beam polarisation is one of the strengths of the LC projects. Comparison of theoretical predictions involving parity-violation with future experimental data is regarded as another powerful tool for confirming or disproving the existence of some beyond the SM scenarios, such as those involving right-handed weak currents and/or new massive gauge bosons.

The plan of the rest of the paper is as follows. In the next Section, we describe the calculation. Then, in Sect. 4, we present some numerical results. We conclude in Sect. 5.

3. Calculation

Since we are considering weak corrections that can be identified via their induced parity-violating effects and since we wish to apply our results to the case of polarised electron and/or positron beams, it is convenient to work in terms of helicity matrix elements (MEs). Thus, we define the helicity amplitudes $\mathcal{A}_{\lambda_1, \lambda_2, \sigma}^{(G)}$ for a gauge boson of type G (hereafter, a virtual photon γ^* or a Z -boson) of helicity λ_1 decaying into a gluon with helicity λ_2 , a massless quark with helicity σ and a massless antiquark with opposite helicity⁴. Since the photon is off-shell, it can have a longitudinal polarisation component, so that the helicity λ_1 always takes three values, $\pm 1, 0$, for both the γ^* and Z gauge vectors⁵, whereas λ_2 and σ can only be equal to ± 1 .

The general form of these amplitudes may be written as

$$\mathcal{A}_{\lambda_1, \lambda_2, \sigma}^{(G)} = \bar{u}(p_2) \Gamma \frac{(1 + \sigma \gamma^5)}{2} v(p_1), \quad (3.1)$$

where p_1 and p_2 are the momenta of the outgoing antiquark and quark respectively and Γ stands for a sum of strings of Dirac γ -matrices with coefficients, which, beyond tree level, involve integrals over loop momenta. Since the helicity σ of the fermions is conserved the strings must contain an odd number of γ -matrices. Repeated use of the Chisholm

⁴Note that all interactions considered here preserve the helicity along the fermion line, including those in which Goldstone bosons appear inside the loop, since these either occur in pairs or involve a mass insertion on the fermion line.

⁵These helicities, wherein $\pm 1(0)$ are(is) transverse(longitudinal), are defined in a frame in which the particle is *not* at rest, so that a fourth possible polarisation in the direction of its four-momentum is irrelevant since its contribution vanishes by virtue of current conservation.

identity⁶ means that Γ can always be expressed in the form

$$\Gamma = C_1 \gamma \cdot p_1 + C_2 \gamma \cdot p_2 + C_3 \gamma \cdot p_3 + C_4 \sqrt{Q^2} \gamma \cdot n, \quad (3.2)$$

where p_3 is the momentum of the outgoing gluon, $Q^2 = (p_1 + p_2 + p_3)^2$ is the square momentum of the gauge boson, and n is a unit vector normal to the momenta of the jets, more precisely:

$$n_\mu = \frac{1}{\sqrt{2} p_1 \cdot p_2 p_1 \cdot p_3 p_2 \cdot p_3} \varepsilon_{\mu\nu\rho\sigma} p_1^\nu p_2^\rho p_3^\sigma. \quad (3.3)$$

The coefficient functions C_i depend on the helicities $\lambda_1, \lambda_2, \sigma$ as well as the energy fractions x_1 and x_2 of the antiquark and quark in the final state, i.e.,

$$x_i = \frac{2E_i}{\sqrt{s}} \quad (i = 1, 2), \quad (3.4)$$

and on all the couplings and masses of particles that enter into the relevant perturbative contribution to the amplitude.

For massless fermions the MEs of the first two terms of eq. (3.2) vanish, and we are left with

$$\begin{aligned} \mathcal{A}_{\lambda_1, \lambda_2, \sigma}^{(G)} &= C_3 \bar{u}(p_2) \gamma \cdot p_3 \frac{(1 + \sigma\gamma^5)}{2} v(p_1) + C_4 \sqrt{Q^2} \bar{u}(p_2) \gamma \cdot n \frac{(1 + \sigma\gamma^5)}{2} v(p_1), \\ &= C_3 Q^2 \sqrt{(1-x_1)(1-x_2)} - i\sigma C_4 Q^2 \sqrt{x_1 + x_2 - 1}. \end{aligned} \quad (3.5)$$

The relevant coefficient functions C_3 and C_4 are scalar quantities and can be projected on a graph-by-graph basis using the projections

$$C_3 = \text{Tr} \left(\Gamma \gamma \cdot v \frac{(1 + \sigma\gamma^5)}{2} \right), \quad (3.6)$$

where v is the vector

$$v = \frac{(1-x_2)p_1 + (1-x_1)p_2 - (x_1+x_2-1)p_3}{2Q^2(1-x_1)(1-x_2)},$$

and

$$C_4 = -\frac{1}{2\sqrt{Q^2}} \text{Tr} \left(\Gamma \gamma \cdot n \frac{(1 + \sigma\gamma^5)}{2} \right). \quad (3.7)$$

At tree level the helicity amplitudes are only functions of x_1, x_2 , the EW couplings $g_j^{(G)}$ of the (anti)quark of type j (proportional to $g_W \equiv \sqrt{4\pi\alpha_{EW}}$, with $\alpha_{EW} = \alpha_{EM}/\sin^2\theta_W$, and carrying information on both helicity and flavour of the latter) to the relevant gauge

⁶This identity is only valid in four dimensions. In our case, where we do not have infrared (i.e., soft and collinear) divergences, it is a simple matter to isolate the ultraviolet divergent contributions, which are proportional to the tree-level MEs, and handle them separately. However, in d dimensions one needs to account for the fact that there are $2^{d/4}$ helicity states for the fermions and $(d-2)$ for the gauge bosons. The method described here will not correctly trap terms proportional to $(d-4)$ in coefficients of divergent integrals. It is probably for this reason that the formalism of Ref. [67] is considerably more cumbersome than that presented here.

boson and the QCD coupling $g_S \equiv \sqrt{4\pi\alpha_S}$. Specifically, in case of massless (anti)quarks (i.e., $m_q = 0$), we have (here, τ^a represents a colour matrix):

$$\begin{aligned}
\mathcal{A}_{1,1,1}^{(G)} &= \mathcal{A}_{-1,-1,-1}^{(G)} = -2ig_j^{(G)} g_S \tau^a \frac{x_1}{\sqrt{(1-x_1)(1-x_2)}}, \\
\mathcal{A}_{1,1,-1}^{(G)} &= \mathcal{A}_{-1,-1,1}^{(G)} = -2ig_j^{(G)} g_S \tau^a \frac{\sqrt{(1-x_1)(1-x_2)}}{x_1}, \\
\mathcal{A}_{0,-1,1}^{(G)} &= \mathcal{A}_{0,1,-1}^{(G)} = -2\sqrt{2}ig_j^{(G)} g_S \tau^a \sqrt{\frac{(1-x_1-x_2)}{x_1}},
\end{aligned} \tag{3.8}$$

with all others being zero. These zero values do not, in general, remain zero in the presence of weak corrections and this can lead to a relative enhancement of the latter, in comparison to QCD effects at the same order.

At one-loop level such helicity amplitudes acquire higher order corrections from the self-energy insertions on the fermions and gauge bosons shown in Fig. 1, from the vertex corrections shown in Fig. 2⁷ and from the box diagrams shown in Fig. 3. As we have neglected here the masses of the final-state quarks, such higher order corrections depend on the ratio Q^2/M_W^2 , where Q^2 is the square momentum of the gauge boson, as well as the EM coupling constant α_{EM} and the weak mixing angle $s_W \equiv \sin\theta_W$ (with $\alpha_{\text{EW}} = \alpha_{\text{EM}}/s_W^2$). Furthermore, in the case where the final state fermions are b -quarks, the loops involving the exchange of a W -boson lead to effects of virtual t -quarks, so that the corrections also depend on the ratio m_t^2/M_W^2 . (It is only in this case that the graphs involving the exchange of the Goldstone bosons associated with the W -boson graphs are relevant.)

The self-energy and vertex correction graphs contain ultraviolet divergences. These have been subtracted using the ‘modified’ Minimal Subtraction ($\overline{\text{MS}}$) scheme at the scale $\mu = M_Z$. Thus the couplings are taken to be those relevant for such a subtraction: e.g., the EM coupling, α_{EM} , has been taken to be $1/128$ at the above subtraction point. Two exceptions to this renormalisation scheme have been the following:

1. the self-energy insertions on external fermion lines, which have been subtracted on mass-shell, so that the external fermion fields create or destroy particle states with the correct normalisation;
2. the mass renormalization of the Z -boson propagator, which has also been carried out on mass-shell, so that the Z mass does indeed refer to the physical pole-mass.

All these graphs are infrared and collinear convergent so that they may be expressed in terms of Passarino-Veltman [39] functions which are then evaluated numerically. The expressions for each of these diagrams have been calculated using FORM [40] and checked by an independent program based on FeynCalc [41]. For the numerical evaluation of the scalar integrals we have relied on FF [42]. A further check on our results has been carried out by setting the polarisation vector of the photon proportional to its momentum and

⁷Note that we also include self-energy and vertex corrections to the incoming $e^+e^- \rightarrow \gamma^*, Z$ current, though we do not show the corresponding graphs.

verifying that in that case the sum of all one-loop diagrams vanishes, as required by gauge invariance. The full expressions for the contributions from these graphs are too lengthy to be reproduced here.

In terms of the helicity MEs we define the following ‘‘spin-matrix’’ tensors, only depending on the polarisation state of the off-shell gauge boson,

$$\mathcal{T}_{\lambda\lambda'}^{(GG')} = \sum_{\lambda_2, \sigma} \mathcal{A}_{\lambda, \lambda_2, \sigma}^{(G)} \left(\mathcal{A}_{\lambda', \lambda_2, \sigma}^{(G')} \right)^\dagger, \quad (3.9)$$

where the (anti)quark and gluon helicities have been summed over. These tensor elements are real at tree level, but in general acquire an imaginary part at one loop arising from the cuts of the loop integrations above the threshold for the production of the internal particles.

Finally, we define the customary nine form-factors, F_1, \dots, F_9 , describing the differential structure of a three-jet final state in terms of the above spin-matrix tensors, as follows:

$$\begin{aligned} F_i = & \frac{\alpha_{\text{EM}}}{512\pi^3} \left[\frac{\left(\eta_A^{L(R)} \right)^2}{Q^2} f_i^{AA} \right. \\ & + \frac{(1 - \lambda_e - 4s_W^2)}{4s_W c_W} \eta_A^{L(R)} \eta_Z^{L(R)} (f_i^{AZ} + f_i^{ZA}) \Re e \left\{ \frac{1}{(Q^2 - M_Z^2 + i\Gamma_Z M_Z)} \right\} \\ & \left. + \left(\frac{1 - \lambda_e - 4s_W^2}{4s_W c_W} \right)^2 Q^2 (\eta_Z^{L(R)})^2 f_i^{ZZ} \Re e \left\{ \frac{1}{(Q^2 - M_Z^2 + i\Gamma_Z M_Z)^2} \right\} \right] \quad (i = 1, \dots, 9) \end{aligned} \quad (3.10)$$

where

$$\begin{aligned} f_1^{GG'} &= \left(\mathcal{T}_{1,1}^{GG'} + \mathcal{T}_{0,0}^{GG'} + \mathcal{T}_{-1,-1}^{GG'} \right), \\ f_2^{GG'} &= \mathcal{T}_{0,0}^{GG'}, \\ f_3^{GG'} &= -2 \Re e \left(\mathcal{T}_{1,1}^{GG'} - \mathcal{T}_{-1,-1}^{GG'} \right), \\ f_4^{GG'} &= -\sqrt{2} \Re e \left(\mathcal{T}_{1,0}^{GG'} + \mathcal{T}_{-1,0}^{GG'} \right), \\ f_5^{GG'} &= -2 \Re e \mathcal{T}_{1,-1}^{GG'}, \\ f_6^{GG'} &= 2\sqrt{2} \Re e \left(\mathcal{T}_{1,0}^{GG'} - \mathcal{T}_{-1,0}^{GG'} \right), \\ f_7^{GG'} &= \sqrt{2} \Im m \left(\mathcal{T}_{0,1}^{GG'} - \mathcal{T}_{0,-1}^{GG'} \right), \\ f_8^{GG'} &= 2 \Im m \mathcal{T}_{1,-1}^{GG'}, \\ f_9^{GG'} &= -2\sqrt{2} \Im m \left(\mathcal{T}_{0,1}^{GG'} + \mathcal{T}_{0,-1}^{GG'} \right), \end{aligned} \quad (3.11)$$

with $\eta_G^{L(R)}$ the weak correction factor to the coupling of the left(right)-handed electron to the gauge boson G and λ_e the helicity of the incoming electron beam (assumed always to be of opposite helicity to the incoming positron beam).

Up to an overall constant, these form-factors are the same as those introduced, e.g., in Refs. [43,44]. The last three (F_7, \dots, F_9) can arise for the first time at the one-loop level,

since they are proportional to the imaginary parts of the spin-matrix. Besides, F_3 , F_6 and F_7 vanish in the parity-conserving limit and can therefore be used as probes of weak interaction contributions to three-jet production. (Moreover, F_3 and F_6 would be exactly zero at tree level if the leading order process were only mediated by virtual photons.)

These form-factors further generate the double differential cross-section for three-jet production in terms of some event shape variable, S , which is in turn related to x_1 , x_2 by some function, s , i.e., $S = s(x_1, x_2)$, and of the polar and azimuthal angles, α , β , between, e.g., the incoming electron beam and the antiquark jet, by⁸

$$\begin{aligned} \frac{d^3\sigma}{dS d\cos\alpha d\beta} = & \int dx_1 dx_2 \delta(S - s(x_1, x_2)) [(2 - \sin^2\alpha) F_1 + (1 - 3\cos^2\alpha) F_2 \\ & + \lambda_e \cos\alpha F_3 + \sin 2\alpha \cos\beta F_4 + \sin^2\alpha \cos 2\beta F_5 + \lambda_e \sin\alpha \cos\beta F_6 \\ & + \sin 2\alpha \sin\beta F_7 + \sin^2\alpha \sin 2\beta F_8 + \lambda_e \sin\alpha \sin\beta F_9]. \end{aligned} \quad (3.12)$$

Note that upon integrating over the antiquark jet angle relative to the electron beam, only the form-factor F_1 survives.

In general, it is not possible to distinguish between quark, antiquark and gluon jets, although the above expression can easily be adapted such that the angles α, β refer to the leading jet. However, (anti)quark jets can be recognised when they originate from primary b -(anti)quarks, thanks to rather efficient flavour tagging techniques (such as μ -vertex devices). We will therefore consider the numerical results for such a case separately.

4. Numerical results

The processes considered here are the following:

$$e^+e^- \rightarrow \gamma^*, Z \rightarrow \bar{q}qg \quad (\text{all flavours}), \quad (4.1)$$

when no assumption is made on the flavour content of the final state, so that a summation will be performed over $q = d, u, c, s, b$ -quarks, and also

$$e^+e^- \rightarrow \gamma^*, Z \rightarrow \bar{b}bg, \quad (4.2)$$

limited to the case of bottom quarks only in the final state. As already intimated, all quarks in the final state of (4.1)–(4.2) are taken as massless⁹. In contrast, the top quark entering the loops in both reactions has been assumed to have the mass $m_t = 175$ GeV. The Z mass used was $M_Z = 91.19$ GeV and was related to the W -mass, M_W , via the SM formula $M_W = M_Z \cos\theta_W$, where $\sin^2\theta_W = 0.232$. (Corresponding widths were $\Gamma_Z = 2.5$ GeV and $\Gamma_W = 2.08$ GeV.) For α_S we have used the two-loop expression for $\Lambda_{\overline{\text{MS}}}^{(n_f=4)} = 200$ MeV throughout (yielding, $\alpha_S(M_Z) = 0.11$).

⁸A qualitative difference between the expressions of the form-factors, F_i ($i = 1, \dots, 9$), used here and those of Refs. [43, 44] is that we do not include the sign of the axial vector coupling of the electron to the exchanged gauge boson in our definitions. In this way the difference between the differential cross-sections for left- and right-handed polarised electron beams is manifest in eq. (3.12).

⁹Mass effects in $e^+e^- \rightarrow \gamma^*, Z \rightarrow \bar{b}bg$ have been studied in [45] and [46].

We systematically neglect higher order effects from EM radiation, including those due to Initial State Radiation (ISR) or beamstrahlung. In fact, although these are known to be non-negligible (especially at LC energies), we expect them to have a similar effect on both the tree-level and one-loop descriptions, hence being irrelevant for our purpose. In this context, we should like to elaborate further on the purely EM corrections to the final state of processes (4.1)–(4.2). Those to the form-factor F_1 have already been calculated, since they can be extracted from the Abelian part of the NLO-QCD corrections (see [38]) by replacing C_F by unity and α_S by α_{EM} . As was pointed out in Ref. [47], these corrections are dominated by a term $\sim \alpha_{EM}\pi/2$ multiplying the tree-level cross-section. This contribution is $\sim 1\%$ and is independent of the jet event shape. A further correction, associated with the Sudakov form-factor, acts in the negative direction and is subdominant away from the two-jet region (i.e., up to values of ~ 0.95 for the Thrust, see below for its definition). There is no reason to believe that these EM corrections would be enhanced for other form-factors.

It is common in the specialised literature to define the n -jet fraction $R_n(y)$ as

$$R_n(y) = \frac{\sigma_n(y)}{\sigma_0}, \quad (4.3)$$

where y is a suitable variable quantifying the space-time separation among hadronic objects and with σ_0 identifying the (energy-dependent) Born cross-section for $e^+e^- \rightarrow \bar{q}q$.

For the choice $\mu = \sqrt{s}$ of the renormalisation scale, one can conveniently write the three-jet fraction in the following form:

$$R_3(y) = \left(\frac{\alpha_S}{2\pi}\right) A(y) + \left(\frac{\alpha_S}{2\pi}\right)^2 B(y) + \dots, \quad (4.4)$$

where the coupling constant α_S and the functions $A(y)$ and $B(y)$ are defined in the \overline{MS} scheme. An experimental fit of the $R_n(y)$ jet fractions to the corresponding theoretical prediction is a powerful way of determining α_S from multi-jet rates.

Through order $\mathcal{O}(\alpha_S)$ processes (4.1)–(4.2) are the leading order (LO) perturbative contributions to the corresponding three-jet cross-section¹⁰, as defined via eqs. (4.3)–(4.4). The LO terms, however, receive higher order corrections from both QCD and EW interactions and we are concerned here with the next-to-leading order (NLO) ones only. Whereas at LO all the contributions to the three-jet cross-section come from the tree-level parton process $e^+e^- \rightarrow \bar{q}qg$ (which contributes to the $A(y)$ function above), at NLO the QCD contributions to the three-jet rate (hereafter, denoted by NLO-QCD) are due to two sources. First, the real emission diagrams for the processes $e^+e^- \rightarrow q\bar{q}gg$ and $e^+e^- \rightarrow q\bar{q}Q\bar{Q}$, in which one of the partons is ‘unresolved’. This can happen when one has either two collinear partons within one jet or one soft parton outside the jet. Both these contributions are (in general, positively) divergent. Thanks to the Bloch-Nordsieck [48] and Kinoshita-Lee-Nauenberg [49] theorems, these collinear and soft singularities are cancelled at the same order in α_S by the divergent contributions (generally negative) provided by the second source, namely, the virtual loop graphs. Therefore, after renormalising the coupling constant α_S , a finite three-jet cross-section is obtained and the function $B(y)$ accounts for

¹⁰Hereafter, perturbative contributions are referred to relatively to the $\mathcal{O}(\alpha_{EM}^2)$ two-jet rate.

the above-mentioned three- and four-parton QCD contributions¹¹. While the EM component of the EW corrections may be treated on the same footing as the QCD one (with the additional photon playing the role of a second gluon), the weak corrections of interest (hereafter, labelled as NLO-W) only contribute to three-parton final states. Hence, in order to account for the latter, it will suffice to make the replacement

$$A(y) \rightarrow A(y) + A_W(y) \quad (4.5)$$

in eq. (4.4).

The decision as to whether two hadronic objects are unresolved or otherwise is usually taken through the application onto the hadronic final state of a so-called ‘jet clustering algorithm’, wherein the number of *clusters*¹² is reduced one at a time by combining the two most (in some sense) nearby ones. The joining procedure is stopped by testing against some criterion and the final clusters are called jets.

As jet clustering schemes¹³, we have used a selection of the ‘binary’ ones, in which only two objects are clustered together at any step. Given two clusters labelled as i and j , the measure of their ‘distance’ is normally denoted by y_{ij} and the minimal separation allowed by y_{cut} . The algorithms are the following: the JADE (J) one [51], which uses as a measure of separation the quantity

$$y_{ij}^{\text{J}} = \frac{2E_i E_j (1 - \cos \theta_{ij})}{s}; \quad (4.6)$$

the Durham (D) [52] and the Cambridge (C) [53] ones, both using¹⁴

$$y_{ij}^{\text{D}} \equiv y_{ij}^{\text{C}} = \frac{2 \min(E_i^2, E_j^2) (1 - \cos \theta_{ij})}{s}; \quad (4.7)$$

the Geneva (G) one [55], for which one has

$$y_{ij}^{\text{G}} = \frac{8 E_i E_j (1 - \cos \theta_{ij})}{9 (E_i + E_j)^2}. \quad (4.8)$$

In eqs. (4.6)–(4.8), E_i and E_j are the energies and θ_{ij} the angular separation of any pair ij of clusters in the final state. The choice of these particular schemes has a simple motivation. The D and C ones are different versions of ‘transverse-momentum’ based algorithms, whereas the J and G ones use an ‘invariant-mass’ measure (see [54] for a review). In fact, these two categories are those that have so far been employed most in phenomenological studies of jet physics in electron-positron collisions, with the former

¹¹In order to calculate these, we make use here of a program based on Ref. [50].

¹²Here and in the following, the word ‘cluster’ refers to hadrons or calorimeter cells in the real experimental case, to partons in the theoretical perturbative calculations and also to intermediate jets during the clustering procedure.

¹³We acknowledge here the well admitted abuse of referring to the various jet ‘finders’ both as algorithms and as schemes, since the last term was originally intended to identify the composition law of four-momenta when pairing two clusters: in our case, $p_{ij}^\mu = p_i^\mu + p_j^\mu$.

¹⁴The Cambridge algorithm in fact only modifies the clustering procedure of the Durham jet finder and the two implementations coincide for $n \leq 3$ parton final states.

gradually overshadowing the latter, thanks to their reduced scale dependence in higher order QCD (e.g., in the case of the $\mathcal{O}(\alpha_S^2)$ three- [54] – [56] and $\mathcal{O}(\alpha_S^3)$ four-jet rates [57]) and to smaller hadronisation effects in the same contexts (see Refs. [54, 55]).

Fig. 4 displays the $A(y)$, $-A_W(y)$ and $B(y)$ coefficients entering eqs. (4.4)–(4.5), as a function of $y(\equiv y_{\text{cut}})$ for the four above jet algorithms at $\sqrt{s} = M_Z$ ¹⁵. A comparison between $A(y)$ and $A_W(y)$ reveals that the NLO-W corrections are negative and remain indeed at the percent level, i.e., of order $\frac{\alpha_{\text{EM}}}{2\pi s_W^2}$ without any logarithmic enhancement (since $\sqrt{s} \approx M_W, M_Z$). They give rise to corrections to $\sigma_3(y)$ of -1% , and thus are generally much smaller than the NLO-QCD ones. In this context, no systematic difference is seen with respect to the choice of jet clustering algorithm, over the typical range of application of the latter at $\sqrt{s} = M_Z$ (say, $y_{\text{cut}} \gtrsim 0.005$ for D, C and $y_{\text{cut}} \gtrsim 0.01$ for G, J).

As already mentioned, it should now be recalled that jets originating from b -quarks can efficiently be distinguished from light-quark jets. Besides, the b -quark component of the full three-jet sample is the only one sensitive to t -quark loops in all diagrams of Figs. 1–3, hence one may expect somewhat different effects from weak corrections to process (4.2) than to (4.1) (the residual dependence on the $Z\bar{q}q$ couplings is also different). This is confirmed by Fig. 5, where we present the total cross section at $\sqrt{s} = M_Z$ for $e^+e^- \rightarrow \gamma^*, Z \rightarrow \bar{b}bg$ as obtained at LO and NLO-W, for our usual choice of jet clustering algorithms and separations. A close inspection of the plots reveals that NLO-W effects can reach the $\sim -2.0\%$ level or so.

In view of these percent effects being well above the error estimate expected at a future high-luminosity LC running at the Z pole, it is then worthwhile to further consider the effects of NLO-W corrections to some other ‘infrared-safe’ jet observables typically used in the determination of α_S , the so-called ‘shape variables’ [58]. A representative quantity in this respect is the Thrust (T) distribution [59]. This is defined as the sum of the longitudinal momenta relative to the (Thrust) axis n_T chosen to maximise this sum, i.e.:

$$\text{T} = \max \frac{\sum_i |\vec{p}_i \cdot \vec{n}_T|}{\sum_i |\vec{p}_i|}, \quad (4.9)$$

where i runs over all final state clusters. This quantity is identically one at Born level, getting the first non-trivial contribution through $\mathcal{O}(\alpha_S)$ from events of the type (4.1)–(4.2). Also notice that any other higher order contribution will affect this observable. Through $\mathcal{O}(\alpha_S^2)$, for the choice $\mu = \sqrt{s}$ of the renormalisation scale, the T distribution can be parametrised in the following form:

$$(1 - \text{T}) \frac{d\sigma}{d\text{T}} \frac{1}{\sigma_0} = \left(\frac{\alpha_S}{2\pi}\right) A^{\text{T}}(\text{T}) + \left(\frac{\alpha_S}{2\pi}\right)^2 B^{\text{T}}(\text{T}). \quad (4.10)$$

Again, the replacement

$$A^{\text{T}}(\text{T}) \rightarrow A^{\text{T}}(\text{T}) + A_W^{\text{T}}(\text{T}) \quad (4.11)$$

accounts for the inclusion of the NLO-W contributions.

¹⁵Notice that $A(y)$ and $A_W(y)$ for the C scheme are identical to those for the D one (recall the previous footnote).

We plot the terms $(\frac{\alpha_S}{2\pi}) A^T(\mathbb{T})$, $(\frac{\alpha_S}{2\pi}) A_W^T(\mathbb{T})$ and $(\frac{\alpha_S}{2\pi})^2 B^T(\mathbb{T})$ in Fig. 6, always at $\sqrt{s} = M_Z$, alongside the relative rates of the NLO-QCD and NLO-W terms with respect to the LO contribution. Here, it can be seen that the NLO-W effects can reach the level of -1% or so and that they are fairly constant for $0.7 \lesssim \mathbb{T} \lesssim 1$. For the case of b -quarks only, similarly to what seen already for the inclusive rates, the NLO-W corrections are larger, as they can reach the -1.6% level.

The ability to polarise electron (and possibly, positron) beams joined with the high luminosity available render future LCs a privileged environment in which to test the structure of hadronic samples. As noted earlier, differential spectra may well carry the distinctive hallmark of some new and heavy strongly interactive particles (such as squarks and gluinos in Supersymmetry), whose rest mass is too large for these to be produced in pairs as real states but that may enter as virtual objects into multi-jet events. Similar effects may however also be induced by the NLO-W corrections tackled here. Both could well be isolated in one or more of the nine form-factors given in eq. (3.10). As already intimated in the previous Section, F_7 to F_9 are identically zero at LO¹⁶, even prior to any integration in α, β and/or averaging over the e^+e^- helicities. Besides, F_7 would remain zero unless corrections involve parity-violating interactions whereas F_3, F_6 and F_9 would not contribute for unpolarised beams. As for F_1, \dots, F_6 , we should mention that the NLO-W corrections to the corresponding tree-level distributions were found to be $\lesssim 1.2(2.0)\%$ for left-(right-)handed incoming electrons¹⁷.

Observables where such effects would immediately be evident are what we call the ‘unintegrated’ (or ‘oriented’) Thrust distributions associated to each of the form-factors in eq. (3.12) (wherein $S = \mathbb{T}$). In Fig. 7, we present the $F_i \equiv F_i(\mathbb{T})$ terms appearing in that expression, each divided by σ_0 (for consistency with the previous plots), alongside the absolute value of the relative size of the NLO-W corrections with respect to the LO case, for the form-factors F_1, \dots, F_6 , which are non-zero at the Born level. For the latter, NLO-W corrections can be either positive or negative, depending on the form-factor being considered, and can be as large as $\pm 4\%$ or so (in the case of F_3 and F_6).

5. Conclusions

On the basis of our numerical findings in the previous Section, we should like to conclude as follows.

- At $\sqrt{s} = M_Z$, the size of the NLO-W corrections to three-jet rates is rather small, of order percent or so, hence confirming that determinations of α_S at LEP1 and SLC are stable in this respect and that the SM background to parity-violating effects possibly induced by new physics is well under control. In contrast, NLO-W effects ought to be included in the case of future high-luminosity LCs running at the Z pole, such as

¹⁶This is strictly true only for massless quarks, as, for $m_q \neq 0$, Ref. [43] has shown that F_9 becomes non-zero.

¹⁷For reasons of space we refrain from presenting here the NLO-W dependence of F_1, \dots, F_6 in term of x_1 and x_2 . The files can be requested from the authors.

GigaZ, where the accuracy of α_S measurements from jet rates is expected to reach the 0.1% level.

- Exclusive observables in three-jet events are also affected by similar NLO-W effects: e.g., the Thrust distribution, as representative of the so-called ‘infrared safe’ quantities. The experimental error expected at LCs in the determination of α_S from such quantities at $\sqrt{s} = M_Z$ is again of the order of 0.1% (or even smaller), so that the inclusion of NLO-W effects in the corresponding theory predictions is then mandatory.
- Effects from NLO-W corrections are somewhat larger in the case of b -quarks in the final state, in comparison to the case in which all flavours are included in the hadronic sample, because of the presence of the top quark in the one-loop virtual contributions.
- Since the exploitation of beam polarisation effects will be a key feature of experimental analyses of hadronic events at future LCs, we have computed the full differential structure of three-jet processes in the presence of polarised electrons and positrons, in terms of the energy fractions of the two leading jets and of two angles describing the final state orientation. The cross-sections were then parametrised by means of nine independent form-factors, the latter presented as a function of Thrust at fixed angles. Three of these form-factors carry parity-violating effects which cannot then receive contributions from ordinary QCD. For the two that are non-zero at LO, the NLO-W corrections were found as large as 4%. Such higher-order weak effects should appropriately be subtracted from hadronic samples in the search for physics beyond the SM.
- All our results were presented for the case of the factorisable NLO-W effects, i.e., for corrections to the initial and final states only. Whereas these should be sufficient to describe adequately the phenomenology of three-jet events at LEP1, SLC and GigaZ energies, at TeV energy scales one expects comparable effects due to the non-factorisable corrections, in which weak gauge bosons connect via one-loop diagrams electrons and positrons to quarks and antiquarks. Their computation is currently in progress and we will report on it in due course.

Acknowledgements

EM and DAR are grateful to the CERN Theory Division and SM to the KEK Theory Division for hospitality while part of this work was been carried out. SM and DAR are grateful to John Ellis for illuminating discussions during the early stages of this project. This research is supported in part by a Royal Society Joint Project within the European Science Exchange Programme (Grant No. IES-14468).

References

- [1] K. Abe *et al.*, [The ACFA Linear Collider Working Group], [hep-ph/0109166](#); T. Abe *et al.*, [The American Linear Collider Working Group], [hep-ex/0106055](#); [hep-ex/0106056](#);

- hep-ex/0106057; hep-ex/0106058; J.A. Aguilar-Saavedra *et al.*, [The ECFA/DESY LC Physics Working Group], hep-ph/0106315; G. Guignard (editor), [The CLIC Study Team], preprint CERN-2000-008 (2000).
- [2] M. Kuroda, G. Moulataka and D. Schildknecht, *Nucl. Phys.* **B 350** (1991) 25; G. Degrossi and A. Sirlin, *Phys. Rev.* **D 46** (1992) 3104; A. Denner, S. Dittmaier and R. Schuster, *Nucl. Phys.* **B 452** (1995) 80; A. Denner, S. Dittmaier and T. Hahn, *Phys. Rev.* **D 56** (1997) 117; A. Denner and T. Hahn, *Nucl. Phys.* **B 525** (1998) 27.
 - [3] W. Beenakker, A. Denner, S. Dittmaier, R. Mertig and T. Sack, *Nucl. Phys.* **B 410** (1993) 245; *Phys. Lett.* **B 317** (1993) 622.
 - [4] P. Ciafaloni and D. Comelli, *Phys. Lett.* **B 446** (1999) 278 [hep-ph/9809321].
 - [5] M. Ciafaloni, P. Ciafaloni and D. Comelli, *Phys. Rev. Lett.* **84** (2000) 4810 [hep-ph/0001142].
 - [6] M. Ciafaloni, P. Ciafaloni and D. Comelli, *Phys. Rev. Lett.* **87** (2001) 211802 [hep-ph/0103315].
 - [7] M. Ciafaloni, P. Ciafaloni and D. Comelli, *Nucl. Phys.* **B 613** (2001) 382 [hep-ph/0103316].
 - [8] M. Beccaria, P. Ciafaloni, D. Comelli, F. M. Renard and C. Verzegnassi, *Phys. Rev.* **D 61** (2000) 073005 [hep-ph/9906319].
 - [9] M. Beccaria, P. Ciafaloni, D. Comelli, F. M. Renard and C. Verzegnassi, *Phys. Rev.* **D 61** (2000) 011301 [hep-ph/9907389].
 - [10] M. Beccaria, F. M. Renard and C. Verzegnassi, *Phys. Rev.* **D 63** (2001) 053013 [hep-ph/0010205].
 - [11] M. Beccaria, F. M. Renard and C. Verzegnassi, *Phys. Rev.* **D 63** (2001) 095010 [hep-ph/0007224].
 - [12] M. Beccaria, F. M. Renard and C. Verzegnassi, *Phys. Rev.* **D 64** (2001) 073008 [hep-ph/0103335].
 - [13] A. Denner, talk given at the ‘International Europhysics Conference on High Energy Physics’, Budapest, Hungary, July 12-18, 2001 [hep-ph/0110155].
 - [14] M. Beccaria, S. Prelovsek, F. M. Renard and C. Verzegnassi, *Phys. Rev.* **D 64** (2001) 053016 [hep-ph/0104245].
 - [15] A. Denner and S. Pozzorini, *Eur. Phys. J.* **C 18** (2001) 461 [hep-ph/0010201].
 - [16] A. Denner and S. Pozzorini, *Eur. Phys. J.* **C 21** (2001) 63 [hep-ph/0104127].
 - [17] S. Pozzorini, *Ph.D. Dissertation*, Universität Zürich (2001).
 - [18] E. Accomando, A. Denner and S. Pozzorini, *Phys. Rev.* **D 65** (2002) 073003 [hep-ph/0110114].
 - [19] M. Melles, *Phys. Lett.* **B 495** (2000) 81 [hep-ph/0006077].
 - [20] M. Hori, H. Kawamura and J. Kodaira, *Phys. Lett.* **B 491** (2000) 275 [hep-ph/0007329].
 - [21] W. Beenakker and A. Werthenbach, *Nucl. Phys. Proc. Suppl.* **89** (2000) 88 [hep-ph/0006009].
 - [22] W. Beenakker and A. Werthenbach, *Phys. Lett.* **B 489** (2000) 148 [hep-ph/0005316].
 - [23] W. Beenakker and A. Werthenbach, *Nucl. Phys.* **B 630** (2002) 3 [hep-ph/0112030].

- [24] V. S. Fadin, L. N. Lipatov, A. D. Martin and M. Melles, *Phys. Rev. D* **61** (2000) 094002 [hep-ph/9910338].
- [25] P. Ciafaloni and D. Comelli, *Phys. Lett. B* **476** (2000) 49 [hep-ph/9910278].
- [26] J. H. Kühn, A. A. Penin and V. A. Smirnov, *Eur. Phys. J. C* **17** (2000) 97 [hep-ph/9912503].
- [27] J. H. Kühn, S. Moch, A. A. Penin and V. A. Smirnov, *Nucl. Phys. B* **616** (2001) 286 [hep-ph/0106298].
- [28] M. Melles, *Phys. Rev. D* **63** (2001) 034003 [hep-ph/0004056].
- [29] M. Melles, *Phys. Rev. D* **64** (2001) 014011 [hep-ph/0012157].
- [30] M. Melles, *Phys. Rev. D* **64** (2001) 054003 [hep-ph/0102097].
- [31] M. Melles, *Phys. Rep.* **375** (2003) 219. [hep-ph/0104232].
- [32] M. Melles, *Eur. Phys. J. C* **24** (2002) 193 [hep-ph/0108221].
- [33] J. Layssac and F. M. Renard, *Phys. Rev. D* **64** (2001) 053018 [hep-ph/0104205].
- [34] See, e.g.:
M. Consoli and W. Hollik (conveners), in proceedings of the workshop ‘Z Physics at LEP1’ (G. Altarelli, R. Kleiss and C. Verzegnassi, eds.), preprint CERN-89-08, 21 September 1989 (and references therein).
- [35] V.A. Khoze, D.J. Miller, S. Moretti and W.J. Stirling, *J. High Energy Phys.* **07** (1999) 014.
- [36] G. Dissertori, talk presented at the ‘XXXI International Conference on High Energy Physics’, Amsterdam, 24-31 July 2002, preprint hep-ex/0209070 (and reference therein).
- [37] M. Winter, LC Note LC-PHSM-2001-016, February 2001 (and references therein).
- [38] R.K. Ellis, D.A. Ross and A.E. Terrano, *Nucl. Phys. B* **178** (1981) 421.
- [39] G. Passarino and M.J.G. Veltman, *Nucl. Phys. B* **160** (1979) 151.
- [40] J.A.M. Vermaseren, preprint NIKHEF-00-032 [math-ph/0010025].
- [41] J. Küblbeck, M. Böhm and A. Denner, *Comput. Phys. Commun.* **64** (1991) 165.
- [42] G.J. van Oldenborgh, *Comput. Phys. Commun.* **66** (1991) 1.
- [43] A. Brandenburg, L. Dixon and Y. Shadmi, *Phys. Rev. D* **53** (1996) 1264 [hep-ph/9505355].
- [44] J.G. Körner and G. Schuler, *Z. Physik C* **26** (1985) 559; K. Hagiwara, T. Kuruma and Y. Yamada, *Nucl. Phys. B* **358** (1991) 80.
- [45] A. Ballestrero, E. Maina and S. Moretti, *Phys. Lett. B* **294** (1992) 425; *Nucl. Phys. B* **415** (1994) 265 [hep-ph/9212246].
- [46] G. Rodrigo, A. Santamaria and M. Bilenky, *Phys. Rev. Lett.* **79** (1997) 193 [hep-ph/9703358]; *J. Phys. G* **25** (1999) 1593 [hep-ph/9703360]; preprint FTUV/98-20, IFIC/98-20 [hep-ph/9802359];
G. Rodrigo, preprint ISBN 84-370-2989-9 [hep-ph/9703359]; *Nucl. Phys. Proc. Suppl.* **54 A** (1997) 60 [hep-ph/9609213];
W. Bernreuther, A. Brandenburg and P. Uwer, *Phys. Rev. Lett.* **79** (1997) 189 [hep-ph/9703305];
A. Brandenburg and P. Uwer, *Nucl. Phys. B* **515** (1998) 279 [hep-ph/9708350];
P. Nason and C. Oleari, *Phys. Lett. B* **407** (1997) 57 [hep-ph/9705295]; *Nucl. Phys. B* **521** (1998) 237 [hep-ph/9709360].

- [47] D.A. Ross, *Nucl. Phys.* **B 188** (1981) 109.
- [48] F. Bloch and A. Nordsieck, *Phys. Rev.* **52** (1937) 54.
- [49] T. Kinoshita, *J. Math. Phys.* **3** (1962) 650;
T.D. Lee and M. Nauenberg, *Phys. Rev.* **133** (1964) 1549.
- [50] F.A. Berends, W.T. Giele and H. Kuijf, *Nucl. Phys.* **B 321** (1989) 595; W.T. Giele and E.W.N. Glover, *Phys. Rev.* **D 46** (1992) 1980.
- [51] JADE Collaboration, *Z. Physik* **C 33** (1986) 23;
S. Bethke, *Habilitation thesis*, preprint LBL 50-208 (1987).
- [52] Yu.L. Dokshitzer, contribution cited in the ‘Report of the Hard QCD Working Group’, in Proceedings of the workshop ‘Jet Studies at LEP and HERA’, Durham, December 1990, *J. Phys* **G 17** (1991) 1537;
S. Catani, Yu.L. Dokshitzer, M. Olsson, G. Turnock and B.R. Webber, *Phys. Lett.* **B 269** (1991) 432.
- [53] Yu.L. Dokshitzer, G.D. Leder, S. Moretti and B.R. Webber, *J. High Energy Phys.* **08** (1997) 001.
- [54] S. Moretti, L. Lönnblad and T. Sjöstrand, *J. High Energy Phys.* **08** (1998) 001.
- [55] S. Bethke, Z. Kunszt, D.E. Soper and W.J. Stirling, *Nucl. Phys.* **B 370** (1992) 310; Erratum, preprint hep-ph/9803267.
- [56] M. Bilenky, G. Rodrigo and A. Santamaria, talk given at the IVth International Symposium on Radiative Corrections (RADCOR98), Barcelona, Catalonia, Spain, 8-12 September 1998, preprint FTUV/98-94, IFIC/98-95 [hep-ph/9812433]; contribution to the XXIX International Conference on High Energy Physics, Vancouver, Canada, July 1998, preprint FTUV/98-79, IFIC/98-80 [hep-ph/9811465];
M. Bilenky, S. Cabrera, J. Fuster, S. Marti, G. Rodrigo and A. Santamaria, *Phys. Rev.* **D 60** (1999) 114006.
- [57] Z. Nagy and Z. Trócsányi, *Phys. Rev.* **D 57** (1998) 5793; *ibidem* **D 59** (1999) 014020; Erratum, *ibidem* **D 62** (2000) 099902.
- [58] See, e.g.: Z. Kunszt and P. Nason, (conveners), in proceedings of the workshop ‘Z Physics at LEP1’ (G. Altarelli, R. Kleiss and C. Verzegnassi, eds.), preprint CERN-89-08, 21 September 1989 (and references therein).
- [59] E. Fahri, *Phys. Rev. Lett.* **39** (1977) 1587.
- [60] K. Hagiwara and D. Zeppenfeld, *Nucl. Phys.* **B 313** (1989) 560.
- [61] F.A. Berends, W.T. Giele and H. Kuijf, *Nucl. Phys.* **B 321** (1989) 39.
- [62] N.K. Falck, D. Graudenz and G. Kramer, *Nucl. Phys.* **B 328** (1989) 317.
- [63] Z. Bern, L.J. Dixon, D.A. Kosower and S. Weinzierl, *Nucl. Phys.* **B 489** (1997) 3 [hep-ph/9610370].
- [64] Z. Bern, L.J. Dixon and D.A. Kosower, *Nucl. Phys.* **B 513** (1998) 3 [hep-ph/9708239].
- [65] E.W.N. Glover and D.J. Miller, *Phys. Lett.* **B 396** (1997) 257 [hep-ph/9609474].
- [66] J.M. Campbell, E.W.N. Glover and D.J. Miller, *Phys. Lett.* **B 409** (1997) 503 [hep-ph/9706297].

- [67] L.W. Garland, T. Gehrmann, E.W.N. Glover, A. Koukoutsakis, and E. Remiddi, *Nucl. Phys.* **B 627** (2002) 107 [[hep-ph/0112081](#)]; *Nucl. Phys.* **B 642** (2002) 227 [[hep-ph/0206067](#)].
- [68] See, e.g.: T. Hebbeker, *Phys. Rep.* **217** (1992) 69 (and references therein).

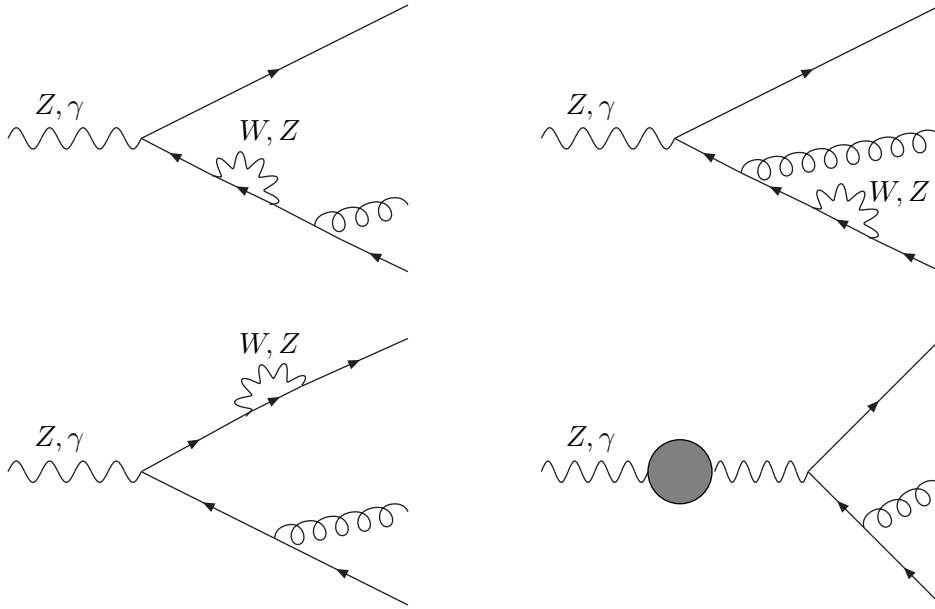


Figure 1: Self-energy insertion graphs. The shaded blob on the incoming wavy line represents all the contributions to the gauge boson self-energy and is dependent on the Higgs mass (hereafter, we will use $M_H = 115$ GeV for the latter). In this and all subsequent figures the graphs in which the exchanged gauge boson is a W -boson is accompanied by corresponding graphs in which the W -boson is replaced by its corresponding Goldstone boson. Since the Yukawa couplings are proportional to the fermion masses, such graphs are only significant in the case of b -quark jets. There is a similar set of diagrams in which the direction of the fermion line is reversed.

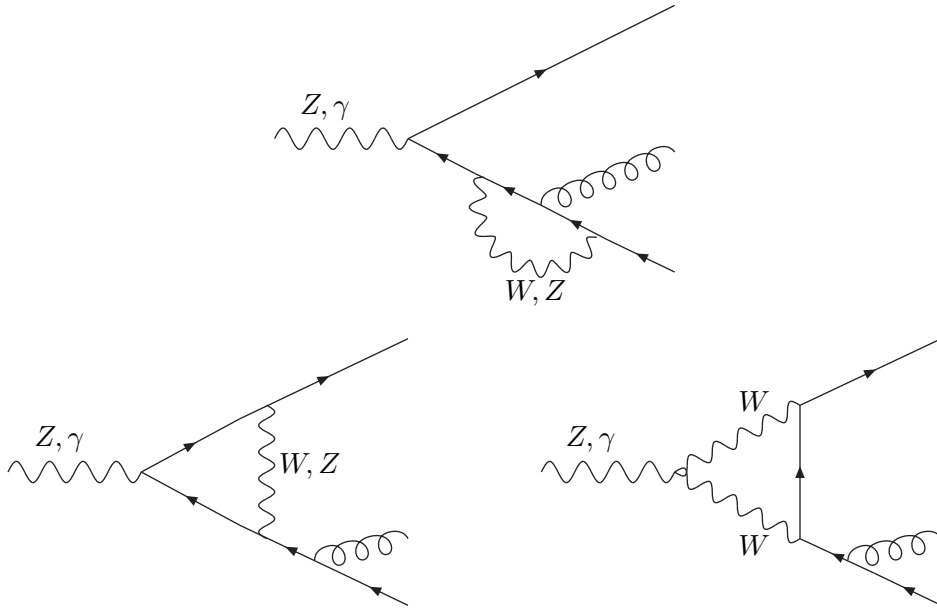


Figure 2: Vertex correction graphs. Again, same considerations as in the previous figure apply for the case of Goldstone bosons and there is a similar set of graphs in which the direction of the fermion line is reversed

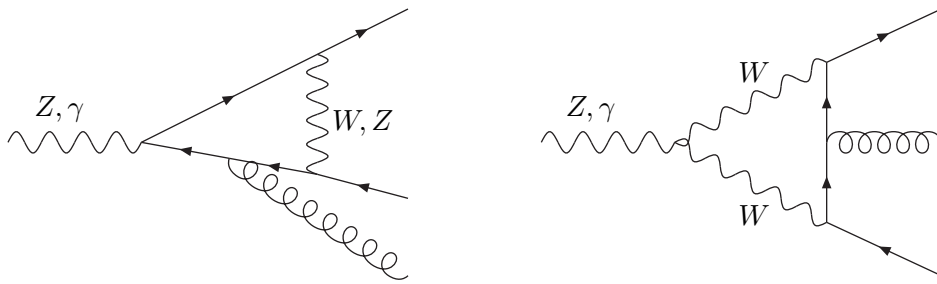


Figure 3: Box graphs. Again, same considerations as in the previous two figures apply for the case of Goldstone bosons. Here, the first graph is accompanied by a similar graph with the direction of the fermion line reversed whereas for the second graph this reversal does not lead to a distinct Feynman diagram.

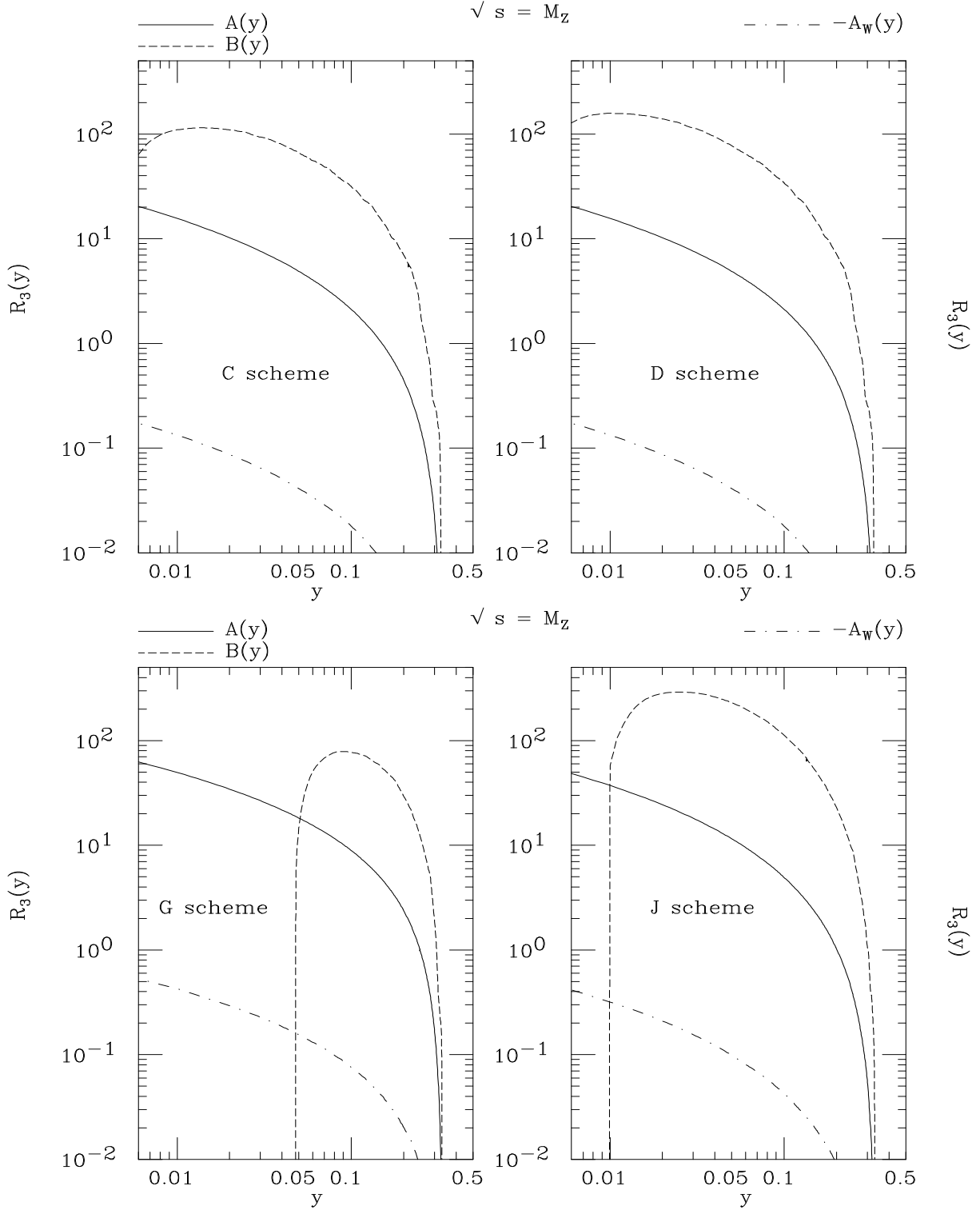


Figure 4: The $A(y)$, $-A_W$ and $B(y)$ coefficient functions of eqs. (4.4)–(4.5) for the Cambridge, Durham, Geneva and Jade jet clustering algorithms, at $\sqrt{s} = M_Z$. (Notice that the $\sim A_W$ term has been plotted with opposite sign for better presentation.)

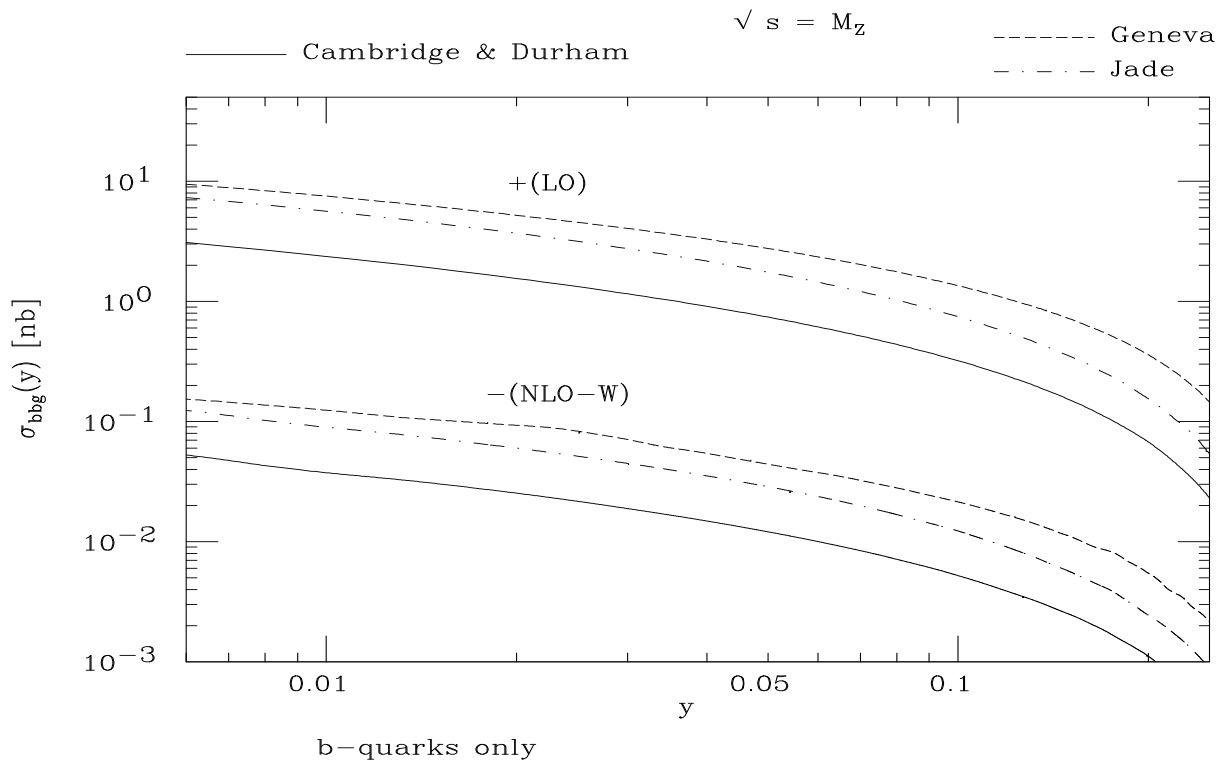


Figure 5: The total cross section for process (4.2) at LO and NLO-W for the Cambridge, Durham, Geneva and Jade jet clustering algorithms, at $\sqrt{s} = M_Z$. (Notice that the NLO-W results have been plotted with opposite sign for better presentation.)

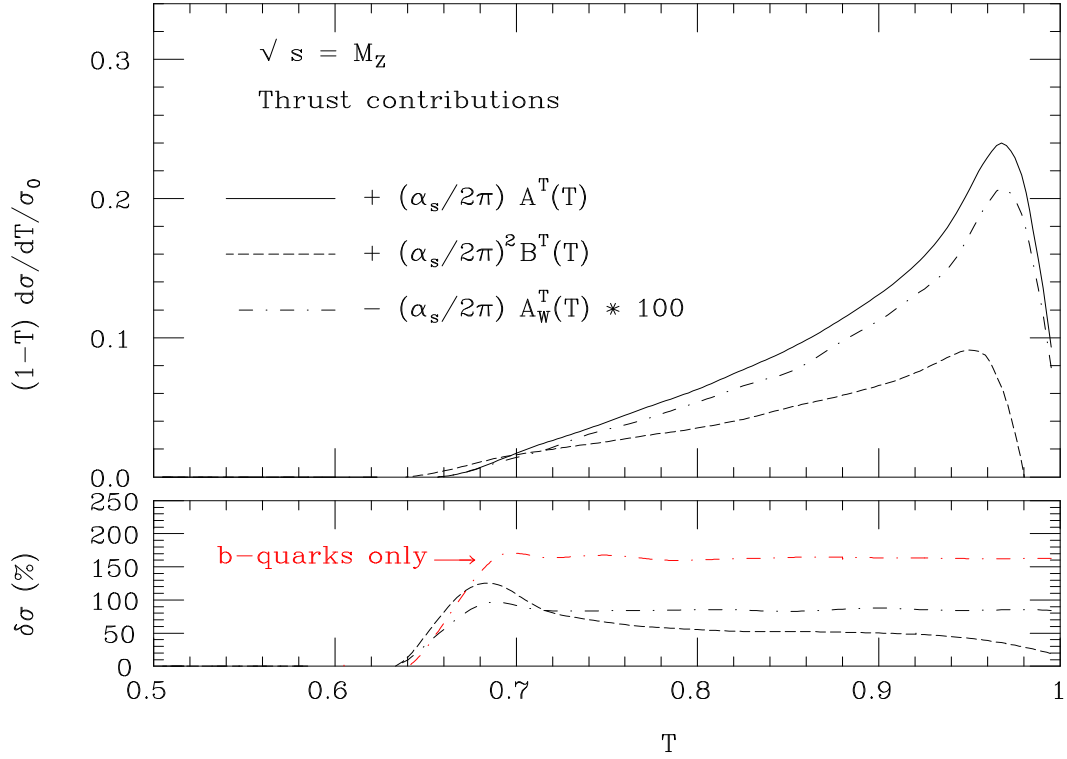


Figure 6: The LO, NLO-QCD and NLO-W contributions to the coefficient functions entering the integrated Thrust distribution, see eq. (4.10), for process (4.1) (top) and the relative size of the two NLO corrections (bottom), at $\sqrt{s} = M_Z$. The correction for the case of b -quarks only is also presented, relative to the LO results for process (4.2). (Notice that the $\sim A_W$ terms have been plotted with opposite sign and multiplied by hundred for better presentation.)

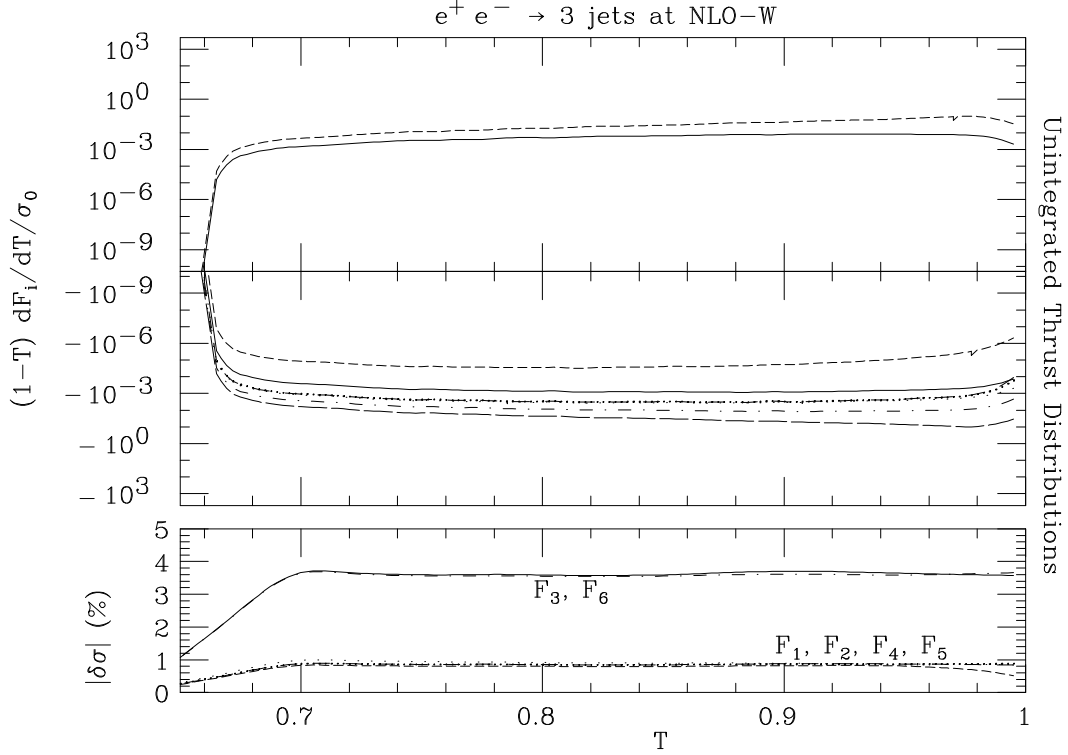


Figure 7: The unintegrated Thrust distributions for the nine component of the cross-section associated to the form-factors in eq. (3.10) for the NLO-W process (4.1) (top and middle) and the relative size of the six components which are non-zero at LO (bottom), at $\sqrt{s} = M_Z$. Labels are as follows: (top) F_4 (solid), F_3 (short-dashed); (middle) F_9 (solid), F_8 (short-dashed), F_7 (dotted), F_6 (dot-dashed), F_5 (dashed), F_2 (fine-dotted), F_1 (long-dashed); (bottom) F_6 (solid), F_5 (short-dashed), F_4 (dotted), F_3 (dot-dashed), F_2 (dashed), F_1 (fine-dotted).